Proceedings of the Seventh International Conference on
Railway Technology: Research, Development and Maintenance
Edited by: J. Pombo
Civil-Comp Conferences, Volume 15, Paper 5.3
Civil-Comp Press, Edinburgh, United Kingdom, 2026
ISSN: 2753-3239, doi: 10.4203/ccc.15.5.3

Influence of Resonant Cavity Structures on Micro-Pressure Waves of High-Speed Maglev Tunnels

J. H. Song, S. Yao, D. Chen, J. Du, G. B. Li and S. Ding

CRRC Qingdao Sifang Co., Ltd., China

Abstract

The high-speed maglev train can operate at speeds exceeding 600 km/h, generating intense micro-pressure waves at tunnel exits when passing through tunnels. To mitigate this issue, a tunnel-installed resonant cavity structure is proposed in this study. Numerical simulations are performed to analyze its aerodynamic mitigation characteristics, and both numerical comparisons and moving model tests are adopted to verify the mitigation effect on micro-pressure waves. The results demonstrate that the resonant cavity can dissipate compression wave energy and reduce the pressure gradient, thus significantly weakening the micro-pressure wave at the tunnel portal. The mitigation efficiencies at 20 m and 50 m from the tunnel exit reach 41.87% and 40.15%, respectively. Moving model tests further validate the accuracy of the optimal scheme determined by numerical simulation.

Keywords: high-speed train, compression wave, micro-pressure wave, resonator, numerical simulation, moving model rig.

1 Introduction

High-speed maglev trains utilize electromagnetic force to overcome gravity and levitate above the guideway. Adopting contactless guidance and drive control technology based on linear motors, such trains break through the limitations of adhesion coefficient, vibration, and noise associated with traditional wheel-rail trains, and can reach operating speeds exceeding 600 km/h. Higher speeds give rise to more severe aerodynamic issues. When a high-speed train enters a tunnel from open air, the annular space formed by the tunnel wall and the train body restricts air flow, compressing the air ahead and generating pressure waves that act on the train body. These waves seriously affect the safety, stability and ride comfort of the train. The micro-pressure wave radiated from the tunnel portal due to compression waves may adversely affect building windows and nearby residents, and even produce explosive noise in severe cases [1-2].

At present, studies on the aerodynamic effects of train-tunnel coupling mainly focus on high-speed wheel-rail trains. Research at home and abroad has shown that the amplitude of the tunnel micro-pressure wave is related to the pressure gradient at the tunnel exit, which is influenced by the generation and propagation of the initial compression wave when the train enters the tunnel, accompanied by physical energy dissipation and nonlinear effects. The basic strategies to reduce micro-pressure waves mainly involve two aspects: the train and the tunnel. For trains, the primary measures are optimizing the cross-sectional area and streamlined head shape [3-6]. For tunnels, common methods include optimizing the tunnel entrance configuration and installing buffer structures such as shafts inside the tunnel. Saito [7] investigated the effects of the cross-sectional area ratio and porosity of a two-stage stepped buffer entrance on the pressure gradient based on acoustic theory. Tao Weiming [8] conducted an in-depth analysis of existing micro-pressure wave mitigation measures, including bell-mouth, linear chamfer, uniform cross-section and enlarged cross-section structures, and obtained the combined mitigation performance of multiple schemes. Wang Tiantian [9] used numerical models and moving model tests to study the mitigation characteristics of enlarged-chamfer buffer structures at the tunnel portal, as well as the influences of structural dimensions and hole numbers, with an optimal mitigation rate of 70.9%. Shi Xianming [10] analyzed the external flow field of a high-speed railway tunnel via numerical simulation and derived the proportional relationship between the micro-pressure wave and the characteristic parameters of the lining size based on pressure gradient variations at monitoring points near the entrance, middle and exit of the tunnel. Zhang Tongtong [11] proposed an internal stepped buffer structure; numerical simulations showed that the pressure gradient mitigation efficiency reached 24.7% when the buffer was placed 60 m from the tunnel entrance, with three-way expansion, a length of 30 m and a cross-sectional area of 150 m^2. Yan Yaguang [12] optimized the bell-mouth buffer structure at the tunnel entrance based on aeroacoustic theory, revealing that the pressure gradient decreased with increasing buffer length, and the peak pressure gradient could be reduced by 63.9%. Li Wenhui [13] simulated the aerodynamic mitigation effects of variable-cross-section tunnels and typical buffer structures, and compared their performance in reducing tunnel pressure waves and micro-pressure waves.

In China, the designed speed of high-temperature superconducting high-speed maglev trains has reached 600 km/h, and the first high-speed maglev system was successfully rolled out in Qingdao. The aerodynamic effects induced by such high speeds when trains pass through tunnels will become even more severe. Mei Yuangui [14] studied the characteristics of micro-pressure waves with and without an open-type buffer structure at the tunnel entrance using three-dimensional numerical simulation, and obtained the critical tunnel lengths for micro-pressure wave mitigation: 33 km for the open-type buffer and 34 km for the shaft structure. Zhang Jie [15] investigated the mitigation effects of portal buffer structures on the initial compression wave gradient and micro-pressure wave amplitude for a 600 km/h maglev train passing through a tunnel, and analyzed the influence of buffer length on the micro-pressure wave amplitude.

The above review indicates that there are relatively few studies on the aerodynamic problems of 600 km/h maglev trains. On the basis of existing research, aiming at the micro-pressure wave at the tunnel portal induced by high-speed maglev trains passing through tunnels, this paper proposes a buffer device using a resonant cavity array arranged in the redundant space of the tunnel. Three-dimensional unsteady compressible Navier–Stokes equations and the SST k-ω turbulence model, combined with overset mesh technology, are adopted to numerically simulate the micro-pressure wave at the tunnel portal when a high-speed maglev train passes through tunnels equipped with different resonant cavity configurations. The mitigation effect of the resonant cavity structure on the micro-pressure wave is analyzed, and the results are verified by moving model tests.

2 Methods

2.1 Geometry

The high-speed maglev train model adopts the real shape of a three-car formation, as shown in Figure 1. It consists of a head car, a middle car and a tail car, with a total length of 81.2 m, a height of 4.2 m and a width of 3.7 m. The train body surface is smoothed without protruding accessories, and the windshields are simplified as fully enclosed windshields.

Figure 1: High-speed maglev train model.

The tunnel model is a single-track tunnel with a T-shaped track beam. The clearance area of the tunnel is 80 m², and the tunnel length is set to 400 m. The resonant cavity structure is arranged starting at 20 m from the tunnel entrance, as illustrated in Figure 2(a). When sound waves propagate into the space formed by the tunnel and the resonant cavities, part of the energy is dissipated due to the acoustic resistance loss of the resonant cavities, thus achieving the effect of noise reduction [16–18]. To minimize the influence on the tunnel blockage ratio, the cavities are installed closely against the inner wall of the tunnel. The propagation model of the resonant cavity is shown in Figure 2(c). Its key parameters include the cross-sectional area A of the connecting tube, the length L of the connecting tube, and the cavity volume V, which determine the natural frequency of the cavity. The connecting tube has a diameter of 0.56 m, corresponding to a cross-sectional area A=0.25 m^2 and a length L=0.4 m. The resonant cavities are distributed along the tunnel length, and

different cavity volumes V correspond to different natural frequencies. Numerical simulations are conducted to compare two schemes of resonant cavity arrays:
Scheme 1 adopts a mixed combination of different cavity volumes, with V ranging from 17.9 m^3 to 111.9 m^3; Scheme 2 uses a uniform cavity volume V=36.5 m^3. The total number of cavities in the 400 m-long tunnel is 28 for Scheme 1 and 47 for Scheme 2, respectively.

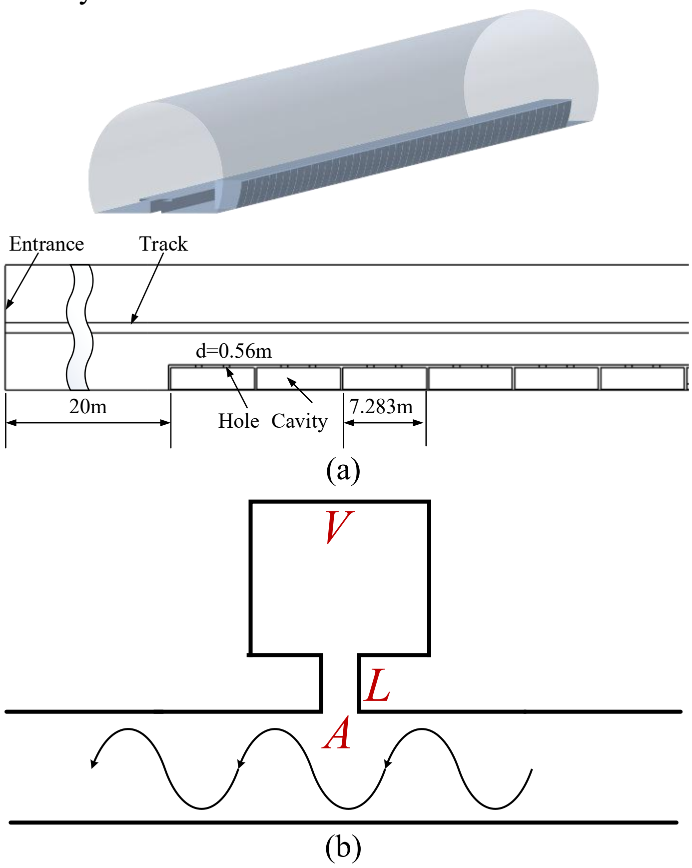

Figure 2: Resonators in the tunnel.

To investigate the effects of the resonant cavity structure on the pressure wave inside the tunnel and the micro-pressure wave at the tunnel portal, pressure monitoring points were deployed on one sidewall of the tunnel and at the tunnel exit. All monitoring points inside the tunnel were positioned at a consistent height of 4 m above the ground. Pressure taps were arranged at 50 m intervals along the inner wall to characterize the propagation of the initial compression wave, including the evolution of its pressure gradient. Monitoring points for micro-pressure waves were placed at distances of 10 m, 20 m, and 50 m from the tunnel exit.

2.2 Computational domain and boundary condition

The overset mesh method, which partitions the flow field into multiple zones, is employed to simulate the pressure wave generated by a maglev train passing through a tunnel. The computational domain is divided into a background zone covering the entire solution domain and an overset zone containing the moving object, so as to realize the relative motion and data exchange between the train and the tunnel. Its accuracy and reliability have been widely recognized in the field of train aerodynamics [19–20].To ensure a fully developed flow field before the train enters the tunnel, the length of the atmospheric zone at both the tunnel entrance and exit is set to 250 m, and the train nose is positioned approximately 100 m away from the tunnel entrance, as shown in Figure 3. Non-reflecting boundary conditions are applied at the inlet and outlet of the atmospheric far field, and a no-slip wall boundary condition is imposed on the train surface.

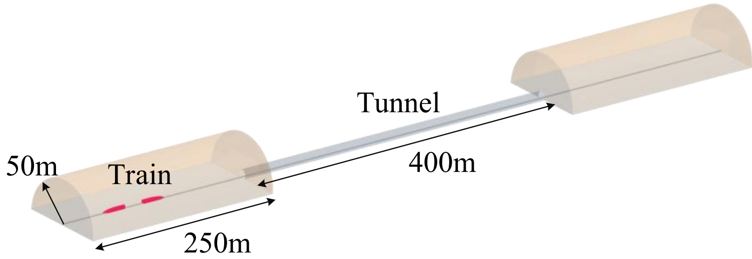

Figure 3: Computional domain

2.3 Mesh generation

In the commercial software STAR-CCM+, the computational domain was meshed volumetrically using the Trimmed mesh approach. The surface mesh size on the train was set to 0.05 m, with a no-slip wall condition applied to the train surface. The wall boundary layer was defined with 10 layers and a growth rate of 1.2. The thickness of the first boundary layer cell was adjusted such that the Y+ value ranged from 100 to 150. Mesh refinement was applied to the operational space of the train and tunnel, as well as to the resonant cavity structures inside the tunnel. The total number of volume cells was approximately 35 million, as illustrated in Figure 4.

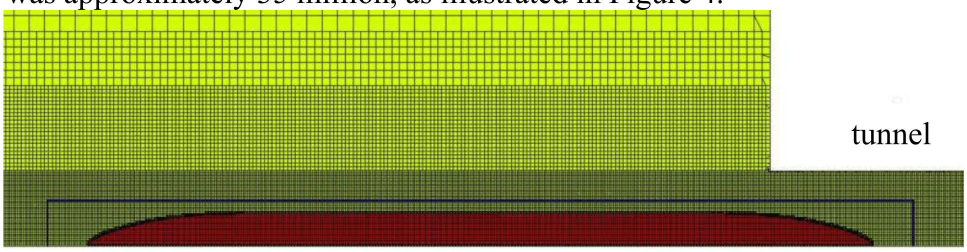

Figure 4: Volume Mesh of simulation model.

The flow field was solved by adopting the three-dimensional, unsteady, and compressible Navier-Stokes equations combined with the SST k-ω turbulence model, where the time step was set to 0.0011 s and 15 iterations were performed for each computational step.

3 Results and discussion

3.1 Pressure wave characteristics for different schemes

Figure 5 presents the pressure fluctuation histories at the tunnel wall for a high-speed maglev train passing through a 400 m-long tunnel at 600 km/h. To illustrate the entire passing process, the figure depicts the propagation of pressure waves induced by the leading and trailing cars entering the tunnel, together with the corresponding train trajectories. Compression waves inside the tunnel are represented by solid black lines, while expansion waves are indicated by dashed black lines; their slopes correspond to the speed of sound and the train speed, respectively.

The train arrives at the tunnel entrance at t=0.623 s, generating a compression wave that propagates at the local speed of sound toward the monitoring point on the tunnel wall, where the pressure begins to rise. As the train enters the tunnel, the pressure at the monitoring point increases continuously. At t=1.698 s, the expansion wave generated by the trailing car entering the tunnel reaches the monitoring point at the local speed of sound, causing the pressure to decrease. Subsequently, as the train passes the monitoring location, the tunnel wall pressure continues to decline.

Installation of the resonant cavity structure inside the tunnel indirectly increases the blockage ratio during train entry, leading to an increase in the pressure wave amplitude on the tunnel wall from 8235 Pa to 8750 Pa, representing a rise of 6.25%. Since Scheme 1 and Scheme 2 impose nearly identical effects on the blockage ratio, the positive peak pressure fluctuations are 8750 Pa and 8787 Pa, and the negative peaks are 9159 Pa and 9011 Pa, respectively, with peak differences below 2%.

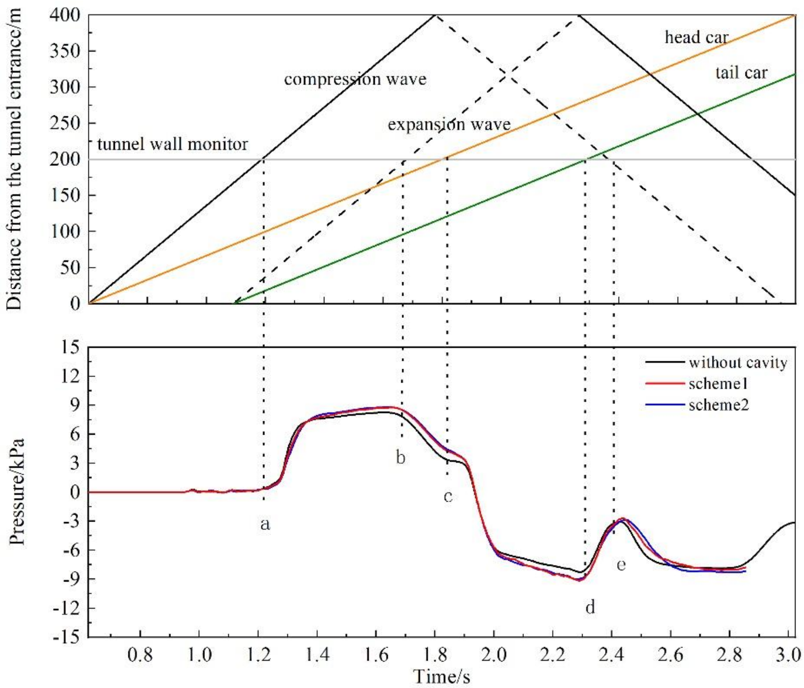

Figure 5: Propagation characteristics of pressure waves under different tunnel structures.

3.2 Micro-pressure wave characteristics for different schemes

Table 1 summarizes the amplitudes of micro-pressure waves at various locations outside the tunnel portal for the two resonant cavity configurations. When the train travels through the single-track tunnel with a clearance area of 80 m² at 600 km/h, the micro-pressure wave amplitudes at 20 m and 50 m from the portal are 898 Pa and 387 Pa, respectively. With the buffer structure of Scheme 1 installed inside the tunnel, the micro-pressure wave amplitudes at the corresponding positions decrease to 589 Pa and 259 Pa, corresponding to reductions of 34.41% and 33.07%, with an average mitigation rate of 33.74%. For Scheme 2, the amplitudes are reduced to 522 Pa and 232 Pa, achieving reductions of 41.87% and 40.05%, with an average mitigation rate of 40.96%. Both resonant cavity configurations exhibit a significant mitigating effect on tunnel portal micro-pressure waves, and Scheme 2 provides superior performance compared with Scheme 1 under the same tunnel length.

Distance from tunnel entrance	10m	20m	50m
without cavity	1392	898	387
scheme1	939	589	259
scheme2	794	522	232

Table 1: Amplitudes of tunnel portal micro-pressure waves in different schemes.

Figure 6 illustrates the time histories of the pressure gradient of the initial compression wave at different monitoring positions along the tunnel wall. During propagation inside the tunnel, the compression wavefront gradually steepens, accompanied by an increase in the pressure gradient. After installing the resonant cavity structures, a portion of the acoustic energy enters the connecting tubes and resonant cavities, where it is absorbed and dissipated. This suppresses the growth of the pressure gradient during the propagation of the initial compression wave, thereby reducing the amplitude of the micro-pressure wave at the tunnel portal. Figure 7 shows the micro-pressure wave and C-weighted noise peak at 20 m outside the tunnel portal for different schemes. In the audible frequency range above 20 Hz, the peak noise level is reduced from 109.5 dB to 105.3 dB and 102.2 dB for the two configurations, respectively.

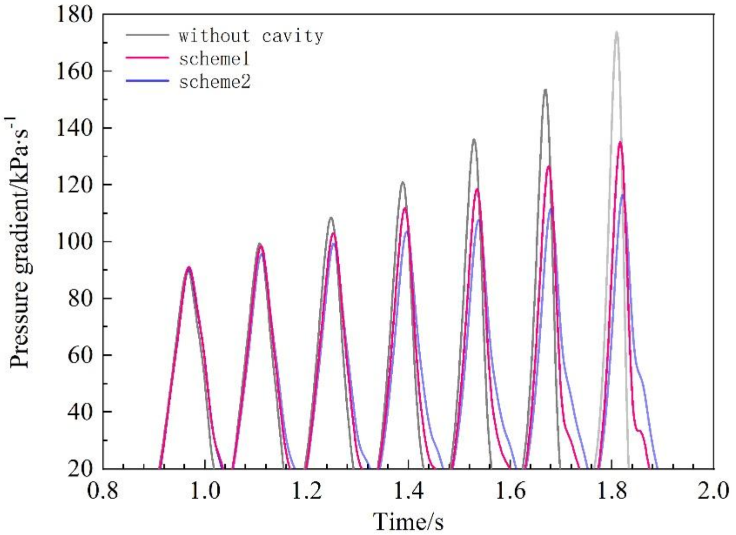

Figure 6: Initial compressive wave pressure gradient of the measurement points at different positions in the tunnel.

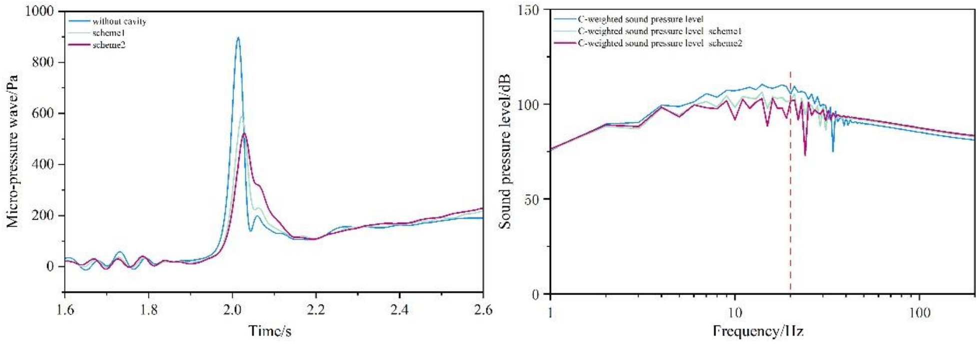

Figure 7: Micro-pressure wave and C-weighted sound pressure level.

3.3 Validation by moving model rig test

A moving model test was conducted to experimentally verify the optimal Scheme 2 of the tunnel resonant cavity structure obtained from numerical simulation. The moving model test was carried out on the moving model test platform in the Key Laboratory of Rail Transit of Central South University. The platform adopts a high-pressure air acceleration system and a graded mechanical braking system, consisting of an acceleration section, a constant-speed section, and a deceleration section, with a total length of 164 m. A 1:20 scaled model vehicle was accelerated by ejection from rest in the acceleration section. After reaching the prescribed test speed, the model vehicle entered the constant-speed section and passed through the tunnel, before being decelerated in the deceleration section and safely stopped within a short distance. The test data were continuously recorded by the measurement system throughout the test, and only data from the constant-speed section were used for analysis. The platform has been certified by CNAS [21]. The experimental model is shown in Fig. 8.


Figure 8: Moving model experimental device.

Figure 9 compares the pressure fluctuations at the tunnel wall and the micro-pressure wave amplitudes at the tunnel portal between the moving model test and numerical simulation. The comparison covers the cases of the train model passing through the plain tunnel and the tunnel equipped with the optimized Scheme 2 resonant cavity structure at 600 km/h. The time histories of the tunnel wall pressure obtained by numerical simulation are in good agreement with those from the moving model test. The maximum error of the pressure peak for the plain tunnel is 5.22%, while that for the tunnel with Scheme 2 resonant cavity is 4.82%. For the micro-pressure wave amplitudes at 20 m and 50 m away from the tunnel portal, the maximum error between simulation and test is 9.1% for the plain tunnel and 9.7% for Scheme 2, both of which are within 10%.

The experimental results demonstrate that the adopted numerical simulation method can accurately predict the aerodynamic effects induced by the train passing through the tunnel, and the resonant cavity structure inside the tunnel has an obvious buffering effect on the micro-pressure wave at the tunnel portal.

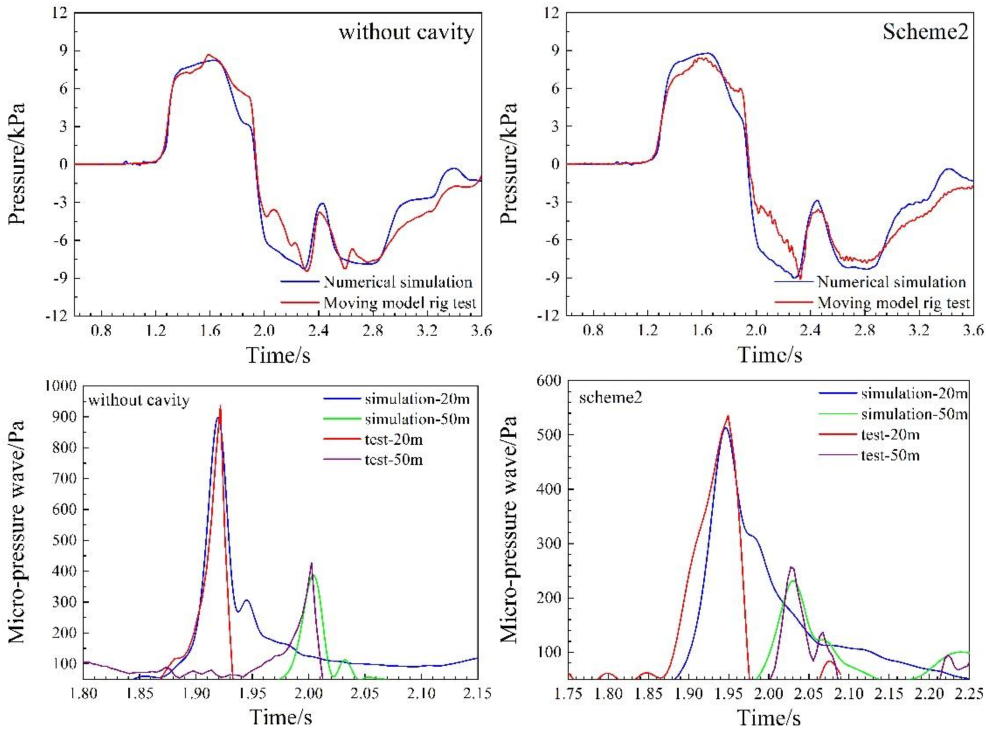

Figure 9: Comparison of moving model rig test and numerical simulation results.

4 Conclusions and Contributions

In this paper, the influence of the resonant cavity structure inside the tunnel on the aerodynamic characteristics of a high-speed maglev train passing through the tunnel is investigated using a combination of numerical simulation and moving model test. The main conclusions are as follows:

1. Installation of the resonant cavity structure in the redundant space of the tunnel reduces the effective clearance area and increases the blockage ratio, resulting in an increase in the pressure on the tunnel wall. When a single train passes through an 80 m² tunnel at 600 km/h, the maximum pressure amplitude at the middle tunnel wall reaches 8750 Pa, representing an increase of 6.25%.

2. The resonant cavity structure significantly dissipates the energy of pressure waves during propagation in the tunnel and suppresses the increase in the pressure gradient of the initial compression wave. At 600 km/h, the average mitigation rate of the micro-pressure wave amplitudes at 20 m and 50 m from the tunnel portal is 40.96%. However, the C-weighted sound pressure level still falls within the range where sonic booms may occur. It is recommended that combined mitigation measures, such as portal hoods and shafts, be adopted to further alleviate the micro-pressure waves.

References

[1] Y.C. Ku, J.H. Rho, S.H. Yun, et al, "Optimal cross-sectional area distribution of a high-speed train nose to minimize the tunnel micro-pressure wave". Struct Multidisc Optim 42, 965-976, 2010, DOI:10.1007/s00158-010-0550-6.

[2] G.W. Yang, Y.J. Wei, G.L. Zhao, "Research progress on the mechanics of high speed rails", Advances in Mechanics, 45: 201507, 2015.

[3] W.B. Ma, Q.L. Zhang, Y.Q. Liu, "Study evolvement of high-speed railway tunnel aerodynamic effect in China", Journal of Traf-fic and Transportation Engineering, 12(4): 25-32, 2012.

[4] J.H. Song, D.L. Guo, G.W. Yang et al, "Experimental investigation on the aerodynamics of tunnel-passing for high speed train with a moving model rig", Journal of Experiments in Fluid Mechanics, 31(05): 39-45, 2017.

[5] Tokuzo Miyachi, Katsuhiro Kikuchi, Michael Hieke, " Multistep train nose for reducing micro-pressure waves ", Vol 520, 2022, DOI: 10.1016/j.jsv.2021.116665

[6] Y. Guo, D.R. Shan, D.L. Guo et al, "Moving model analysis of the initial compression wave in tunnel for high-speed trains", Mechanics in Engineering, 40(5): 495-502, 2018.

[7] S. Saito, T. Fukuda, "Design of a tunnel entrance hood for high-speed trains", Journal of Wind Engineering and Industrial Aerodynamics, 206,2020, DOI: 10.1016/j.jweia.2020.104375

[8] W.M. Tao, "Research on the alleviation effects of micro pressure wave countermeasures at the high speed railway tunnel portal", Journal of Railway Engineering Society, 37(08): 65-70, 2020.

[9] T.T. Wang, C. Hu, Y.F. Gong et al. "Mitigation of micro-pressure wave at 400 km/h railway tunnel exit by oblique enlarged tunnel-hood", Acta Aerodynamica Sinica, 39(5): 151-161, 2021.

[10] X.M. Shi, J. Wu, X.Q. Leng et a, "Influence of added lining on micro pressure wave of high speed railway tunnel portals", Railway Engineering, 57(10): 53-55+59, 2017.

[11] T.T. Zhang, Y.G. Yan, Z.C. Zhao, et al, "Analysis of aerodynamic effects of inter-stepwise buffer structure in high-speed railway tunnel", Journal of Taiyuan University of Technology, 53(4): 779-785, 2022.

[12] Y.G. Yan, Q.S. Yang, J.J. Luo, "Optimizing flared hood of tunnel based on aero acoustics", Journal of Southwest Jiaotong University, 51(05): 832-839, 2016.

[13] W.H. Li, T.H. Liu, M.M. Zhou et al, "Comparative analysis on aerodynamic mitigation effects between tunnels with variable cross-section and typical tunnel hoods", Journal of Central South University(Science and Technology), 53(5): 1572-1581, 2022.
[14] Y.G. Mei, M.H. Li, X. Hu, et al, "Propagation characteristics of initial compression wave in cave and portal micro-pressure waves characteristics when 600km/h maglev train entering tunnels", Journal of Traffic and Transportation Engineering, 21(4): 150-162, 2021.
[15] J. Zhang, Y.G. Wang, S. Han, et al, "Influence of hood length on pressure wave characteristics induced by 600 km/h maglev train passing through tunnel", Journal of Central South University(Science and Technology), 53(5): 1668-1678, 2022.
[16] D.F. Ruan, "The design theory and application on the resonant intake silencer", Chongqing: Chongqing University, 2005
[17] J.A. Tebbutt, M. Vahdati, D. Carolan et al, "Numerical investigation on an array of Helmholtz resonators for the reduction of micro-pressure waves in modern and future high-speed rail tunnel systems". Journal of Sound and Vibration, 400: 606-625, 2017, DOI: 10.1016/j.jsv.2017.04.022
[18] B. Lombard, J. Mercier, "Numerical modeling of nonlinear acoustic waves in a tube connected with Helmholtz resonators", Journal of Computational Physics, 259: 421-443, 2014, DOI: 10.1016/j.jcp.2013.11.036
[19] M.Z. Wang, Y.G. Mei, Y.X. Jia, "Simulation of aerodynamic effects generated by a high-speed train passing through a tunnel with overset grid method", Chinese Journal of Applied Mechanics, 34(03): 589-595+618, 2017.
[20] K.S. Ren. "Preliminary study on aerodynamic effect of hood structure at the entrance of maglev railway tunnel with speed of 600km/h", Lanzhou: Lanzhou Jiaotong University, 2021.
[21] S. Huang, Z.W. Li, M.Z. Yang, et al. "Pressure wave characteristics of high-speed maglev train passing through tunnel groups", Journal of Central South University(Science and Technology), 53(5): 1770-1781, 2022.